$Hg_2(HTe_2O_5)(PO_4)$: A novel phosphate crystal with enhanced birefringence enabled by the synergistic modification of multiple functional groups

Peng-Fei Li,[a,b,c] Chun-Li Hu,[*,a,c] Bo Zhang,[a,b,c] Jiang-Gao Mao[a,c] and Fang Kong[*,a,b,c]

[a] *State Key Laboratory of Functional Crystals and Devices, Fujian Institute of Research on the Structure of Matter, Chinese Academy of Sciences, Fuzhou 350002, P. R. China.*

[b] *College of Chemistry, Fuzhou University, Fuzhou 350108, P. R. China.*

[c] *University of Chinese Academy of Sciences, Beijing 100049, P. R. China.*

[*]Corresponding Authors: clhu@fjirsm.ac.cn; kongfang@fjirsm.ac.cn

Supporting Information

S1. Experimental Section

Materials and Instrumentations.

All the chemicals were obtained from commercial sources and used without further purification: TeO_2 (Adamas-beta, 99.999%), HgO (Aladdin, 99.9%), and H_3PO_4 (Aladdin, ≥85%). (***Caution:*** *HgO is highly toxic, and all operations must be handled with extreme caution, using the appropriate protective equipment and training.*)

Powder X-ray diffraction (PXRD) patterns of $Hg_2(HTe_2O_5)(PO_4)$ was collected on the Miniflex 600 powder X-ray diffractometer using Cu Kα radiation (λ = 1.54186 Å) at room temperature in the angular range of 2θ = 10-70° with a scan step size of 0.02°.

Microprobe elemental analysis was carried out with the aid of a field-emission scanning electron microscope (JSM6700F) outfitted with an energy-dispersive X-ray spectroscope (Oxford INCA).

IR spectra were carried out on a Magna 750 FT-IR spectrometer using KBr as background in the range of 4000–400 cm^{-1} with a resolution of 2 cm^{-1} at room temperature.

The UV-vis-NIR spectra was obtained at 2000–200 nm by a PerkinElmer Lambda 900 spectrophotometer using $BaSO_4$ as the reference, and the reflection spectra were converted into an absorption spectrum using the Kubelka-Munk function. Absorption data was calculated from the diffuse reflection data by the Kubelka-Munk function: $\alpha/S = (1-R)^2/2R$, where α and S represent the absorption coefficient and the scattering coefficient, respectively. The band gap value can be given by extrapolating the absorption edge to the baseline in the α/S vs. energy graph.

Thermogravimetric analyse (TGA) was measured by Netzsch STA 499C installation. The samples about 3.0-5.0 mg were placed in alumina crucibles and heated in 20-1200 °C at a rate of 15 °C/min under N_2 atmosphere.

Birefringence Measurements. The birefringence of $Hg_2(HTe_2O_5)(PO_4)$ was measured by using the polarizing microscope (NIKON ECLIPSE LV100N POL) equipped with a Berek compensator. The wavelength of the light source was 546 nm. Owing to the clear boundary lines of the first-, second-and third-order interference color, the relative error was small enough. Before the scanning, the small and transparent $Hg_2(HTe_2O_5)(PO_4)$ crystal was chosen to measure, in order to improve the accuracy of the birefringence. The thickness of the selected crystal was measured on the polarizing microscope. The formula for calculating the birefringence is listed below:

$$R=|n_e-n_o|\times T=\Delta n \times T$$

Here, R represents the optical path difference, Δn means the birefringence, and T denotes the thickness of the crystal.

Single-crystal X-ray diffraction data was obtained on Agilent Technologies SuperNova dual-wavelength CCD diffractometer with a graphite-monochromated Mo Kα radiation ($\lambda = 0.71073$ Å) at room temperature. Data reduction and cell refinement and were performed with *CrysAlisPro*. The structure was solved by the direct methods and refined by full-matrix least-squares fitting on F^2 using *OLEX2-1.5* crystallographic software package. All non-hydrogen atoms were refined with anisotropic thermal parameters. Hydrogen atoms were located at geometrically calculated positions and refined with isotropic thermal parameters. The structural data were also checked by PLATON and no higher symmetry was found. The detailed crystallographic data for $Hg_2(HTe_2O_5)(PO_4)$ was given in Table S1. The bond lengths were listed in Table S2.

Syntheses

$Hg_2(HTe_2O_5)(PO_4)$ was synthesized by hydrothermal method. A mixture of TeO_2 (159.6 mg, 1 mmol), HgO (324.9 mg, 1.5 mmol), H_3PO_4 (0.15 ml) and H_2O (3 ml) was sealed in an autoclave containing Teflon liner equipped (23 ml), heated at 230 °C for 4320 minutes, and then slowly cooled to room temperature in 4320 minutes. The products were separated by vacuum filtration, washed with alcohol, and dried in air at room temperature. The transparent crystal $Hg_2(HTe_2O_5)(PO_4)$ was obtained in a single pure phase, with a yield of about 36% (based on Te), its purity was confirmed by X-ray diffraction (XRD) studies (Figure S1).

S2. Computational Method

Single-crystal structural data of $Hg_2(HTe_2O_5)(PO_4)$ was used for the theoretical calculations. The electronic structures were performed using a plane-wave basis set and pseudo-potentials within density functional theory (DFT) implemented in the total-energy code CASTEP[1]. For the exchange and correlation functional, we chose Perdew–Burke–Ernzerhof (PBE) in the generalized gradient approximation (GGA)[2]. The interactions between the ionic cores and the electrons were described by the nom conserving pseudopotential[3]. The following valence-electron configurations were considered in the computation: Hg-$5d^{10}5p^66s^2$, Te-$5s^25p^4$, H-$1s^1$, O-$2s^22p^4$ and P-$3s^23p^3$. The numbers of plane waves included in the basis sets were determined by cutoff energy of 750 eV for $Hg_2(HTe_2O_5)(PO_4)$. The numerical integration of the Brillouin zone was performed using Monkhorst-Pack k-point sampling of 4 × 3 × 3. The other parameters and convergent criteria were the default values of CASTEP code.

The calculations of linear optical properties in terms of the complex dielectric function $\varepsilon(\omega) = \varepsilon_1(\omega) + i\varepsilon_2(\omega)$ were made. The imaginary part of the dielectric function ε2 was given in the following equation:

$$\varepsilon^{ij}_2(\omega) = \frac{8\pi^2 h^2 e^2}{(m^2 V)} \sum_k \sum_{cv} (f_c - f_v) \frac{p^i_{cv}(k) p^j_{cv}(k)}{E^2_{vc}} \delta[E_c(k) - E_v(k) - h\omega]$$

The f_c and f_v represent the Fermi distribution functions of the conduction and valence band. The term $p^i_{cv}(k)$ denotes the momentum matrix element transition from the energy level c of the conduction band to the level v of the valence band at the *k*th point in the Brillouin zone (BZ), and *V* is the volume of the unit cell.

The real part $\varepsilon_1(\omega)$ of the dielectric function $\varepsilon(\omega)$ follows from the Kramer–Kronig relationship. All the other optical constants may be derived from $\varepsilon_1(\omega)$ and $\varepsilon_2(\omega)$. For example, the refractive index $n(\omega)$ can be calculated using the following expression[4]:

$$n(\omega) = \left(\frac{1}{\sqrt{2}}\right)\left[\sqrt{\varepsilon_1^2(\omega) + \varepsilon_2^2(\omega)} + \varepsilon_1(\omega)\right]^{1/2}$$

In addition, using the polarizability anisotropy-weighted electron density (PAWED) method, the contributions of constituent groups/atoms to the large birefringence of

$Hg^{I}_2Hg^{II}(Te_2O_4)_2(HPO_4)_2$ can be intuitively displayed and accurately calculated. The PAWED method has been described in detail in our previous work.

Table S1. Summary of crystal data and structural refinements for $Hg_2(HTe_2O_5)(PO_4)$.

Molecular formula	**$Hg_2(HTe_2O_5)(PO_4)$**
Formula Weight	832.36
crystal system	triclinic
space group	*P*-1
Temperature (K)	288.15
F (000)	704.0
a/Å	5.8856(3)
b/Å	7.2589(3)
c/Å	10.1972(4)
α(deg)	81.006(3)
β(deg)	74.483(3)
γ(deg)	82.959(4)
V/Å^3	413.12(3)
Z	2
Dc (g.cm^{-3})	6.691
GOF on F^2	0.996
R_1, $wR_2[I > 2\sigma(I)]^{\alpha}$	$R_1 = 0.0291$, $wR_2 = 0.0543$
R_1, wR_2 (all data)$^{\alpha}$	$R_1 = 0.0351$, $wR_2 = 0.0561$

$^{a}R_1 = \sum||F_o| - |F_c||/\sum|F_o|$, $wR_2 = \{\sum w[(F_o)^2 - (F_c)^2]^2/\sum w[(F_o)^2]^2\}^{1/2}$

Table S2. Calculated bond valences for $Hg_2(HTe_2O_5)(PO_4)$.

Bond	**Bond lengths**	**Bond-valence**	**BVS**
Te(1)-O(1)	1.870(6)	1.335	4.176
Te(1)-O(2)	1.916(6)	1.179	
Te(1)-O(3)	1.969(5)	1.022	
Te(1)-O(6)#1	2.344(6)	0.371	
Te(1)-O(9)#2	2.463(5)	0.269	
Te(2)-O(3)	1.999(5)	0.943	3.802
Te(2)-O(4)	1.880(6)	1.300	
Te(2)-O(5)	1.904(6)	1.218	
Te(2)-O(8)#3	2.375(5)	0.341	
P(1)-O(6)	1.541(6)	1.186	4.696
P(1)-O(7)	1.560(6)	1.126	
P(1)-O(8)	1.539(6)	1.192	
P(1)-O(9)	1.539(6)	1.192	
Hg(1)-O(1)#1	2.639(5)	0.165	1.991 **2.139**
Hg(1)-O(1)#4	2.159(5)	0.603	
Hg(1)-O(4)	2.138(6)	0.638	
Hg(1)-O(5)#4	2.625(6)	0.171	
Hg(1)-O(6)	2.483(6)	0.251	
Hg(1)-O(9)#5	2.643(6)	0.163	
Hg(1)-O(3)	**2.679(6)**	**0.148**	
Hg(2)-O(5)	2.138(6)	0.638	1.532 **2.047**
Hg(2)-O(7)	2.108(6)	0.692	
Hg(2)-O(8)#6	2.564(6)	0.202	
Hg(2)-O(2)	**2.770(5)**	**0.116**	
Hg(2)-O(4)	**2.666(7)**	**0.153**	
Hg(2)-O(4)	**2.805(5)**	**0.105**	
Hg(2)-O(5)	**2.696(6)**	**0.141**	

Bold font: Longer Hg-O bonds were considered.

Symmetry transformations used to generate equivalent atoms:

#1 2-X,1-Y,1-Z; #2 1+X,-1+Y,+Z; #3 1-X,1-Y,2-Z; #4 -1+X,+Y,+Z; #5 -1+X,+Y,+Z; #6 1+X,+Y,+Z

Table S3. State energies (eV) of the lowest conduction band (L-CB) and the highest valence band (H-VB) of $Hg_2(HTe_2O_5)(PO_4)$.

Compound	**k-point**	**L-CB**	**H-VB**
$Hg_2(HTe_2O_5)(PO_4)$	G (0.000, 0.000, 0.000)	2.86903	0
	F (0.000, 0.500, 0.000)	2.75532	-0.03763
	Q (0.000, 0.500, 0.500)	2.83266	-0.16036
	Z (0.000, 0.000, 0.500)	3.01434	-0.13772

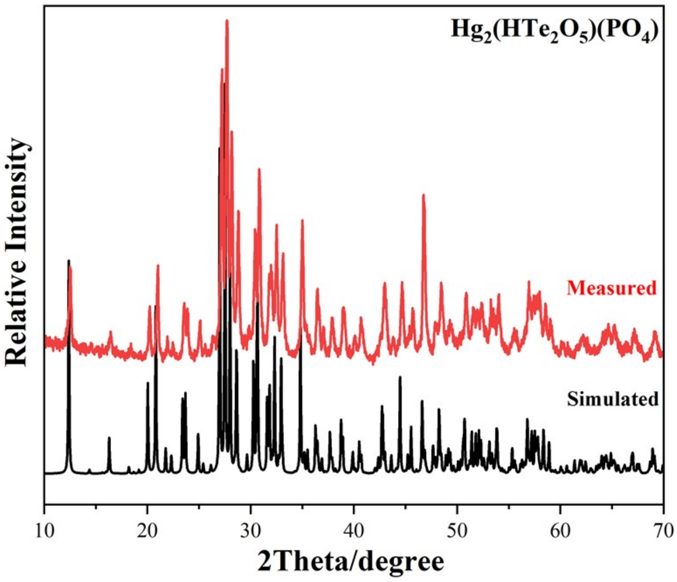

Figure S1. Simulated and experimental powder X-ray diffractometer patterns of $Hg_2(HTe_2O_5)(PO_4)$.

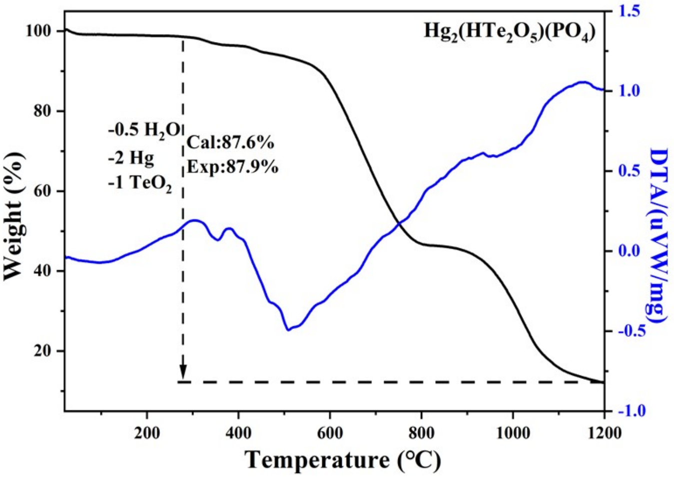

Figure S2. TGA and DTA results of $Hg_2(HTe_2O_5)(PO_4)$.

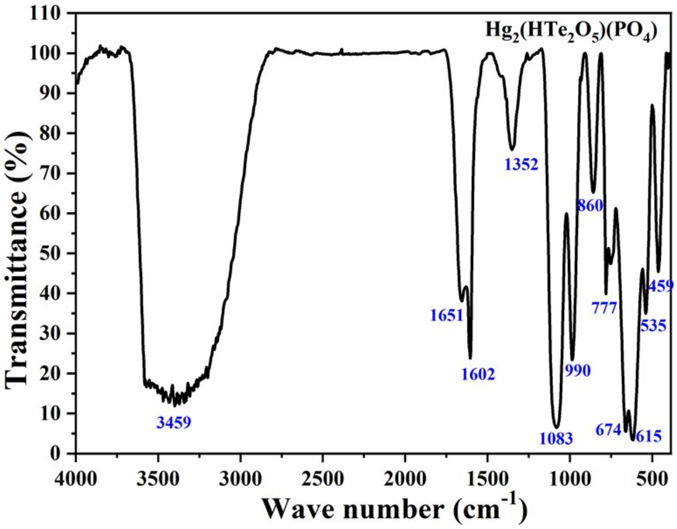

Figure S3. IR spectra of $Hg_2(HTe_2O_5)(PO_4)$.

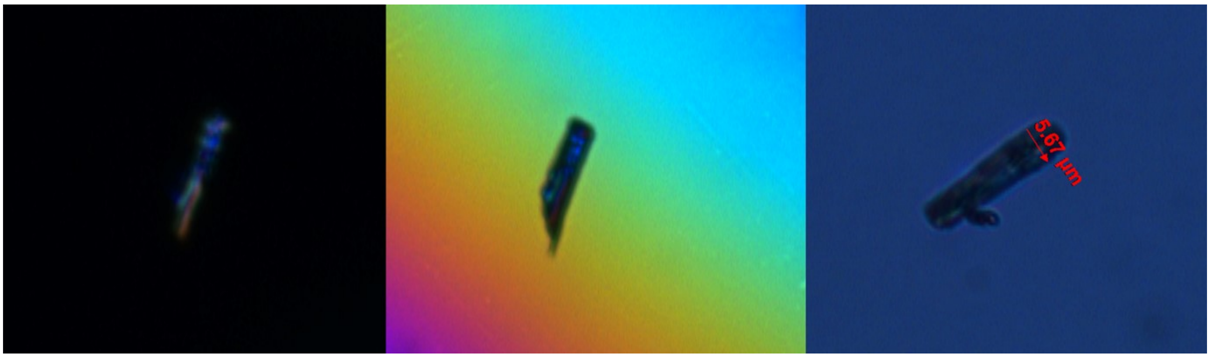

Figure S4. Experimental birefringence of $Hg_2(HTe_2O_5)(PO_4)$ at 546 nm.

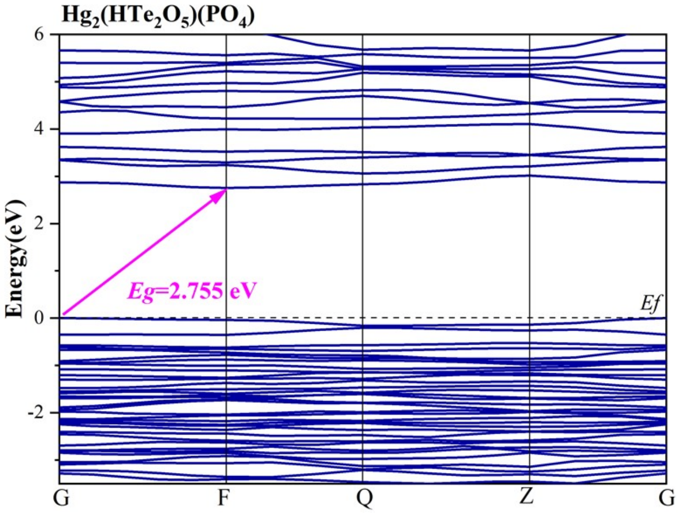

Figure S5. The band structures of $Hg_2(HTe_2O_5)(PO_4)$.

References

1. Segall, M. D.; Lindan, P. J. D.; Probert, M. J.; Pickard, C. J.; Hasnip, P. J.; Clark, S. J.; Payne, M. C., First-principles simulation: ideas, illustrations and the CASTEP code. *Phys-Condens Mat.* **2002,** *14* (11), 2717-2744.
2. Milman, V.; Winkler, B.; White, J. A.; Pickard, C. J.; Payne, M. C.; Akhmatskaya, E. V.; Nobes, R. H., Electronic structure, properties, and phase stability of inorganic crystals: A pseudopotential plane-wave study. *Int. J. Quantum. Chem.* **2000,** *77*, 895-910.
3. Perdew, J. P.; Burke, K.; Ernzerhof, M., Generalized Gradient Approximation Made Simple. *Phys. Rev. Lett.* **1996,** *77* (18), 3865-3868.
4. Vanderbilt, D., Soft self-consistent pseudopotentials in a generalized eigenvalue formalism. *Phys Rev B Condens Matter.* **1990,** *41* (11), 7892-7895.